ACS Medicinal Chemistry Letters

pubs.acs.org/acsmedchemlett Letter

Conjugation Ratio, Light Dose, and pH Affect the Stability of Panitumumab–IR700 for Near-Infrared Photoimmunotherapy

Daiki Fujimura, Fuyuki Inagaki, Ryuhei Okada, Adrian Rosenberg, Aki Furusawa, Peter L. Choyke, and Hisataka Kobayashi*

Cite This: *ACS Med. Chem. Lett.* 2020, 11, 1598–1604

Read Online

ACCESS | Metrics & More | Article Recommendations

ABSTRACT: Near-infrared photoimmunotherapy (NIR-PIT), a newly developed cancer-cell-specific therapy, relies on a monoclonal antibody–photoabsorber conjugate (APC) and is based on a photoinduced ligand release reaction. Local exposure of the tumor to NIR light induces rapid immunogenic necrotic cell death. The molecular properties of APCs, including their stability and aggregation properties, have important implications for the long-term stability and shelf life. In this study, panitumumab was conjugated with IRDye700DX (IR700) as a model for other NIR-PIT agents. Higher IR700-to-mAb conjugation ratios correlated with increased in vitro cell death up to a ratio of 2.5 dye molecules per antibody. Conjugation ratios higher than 2.5 did not improve cell killing activity. APC aggregation was induced in a light-dose-dependent manner. A near-room-level light dose was sufficient to induce aggregation of APCs. Solvent pH lower than 4 induced aggregation, but higher pH did not induce aggregation. The IR700-to-mAb conjugation ratio, light irradiation dose, and solvent pH affect the APC stability and efficacy.

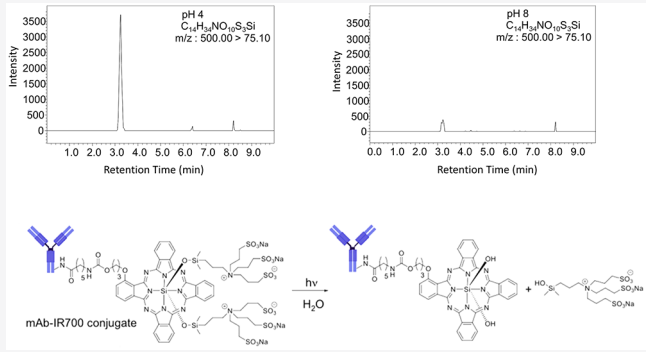

KEYWORDS: *Photoimmunotherapy, antibody–photoabsorber conjugate (APC), aggregation, photostability, pH stability, size-exclusion chromatography (SEC)*

Near-infrared photoimmunotherapy (NIR-PIT) is a newly developed cancer treatment that induces highly cancer-cell-specific cell death. NIR-PIT is based on a monoclonal antibody conjugated to a silica–phthalocyanine dye, IRDye700DX (IR700).[1,2] This antibody–photoabsorber conjugate (APC) is injected, circulates, and binds to the target tumor. Upon exposure to 690 nm NIR radiation, the IR700 on the APC undergoes a ligand release reaction, leading to alterations in its solubility from highly hydrophilic to highly hydrophobic, resulting in a conformational change in the APC–target antigen complex[3] that leads to rapid cell membrane damage and highly immunogenic cell death with blebbing, rapid volume expansion, membrane rupture, and extrusion of cell contents into the extracellular space.[4,5] There are minimal cytotoxic effects in adjacent normal cells.[2] Phase I/II clinical studies of NIR-PIT in patients with inoperable head and neck cancer using cetuximab (anti-EGFR)–IR700 have been completed, and a phase III clinical trial is underway worldwide (https://clinicaltrials.gov/ct2/show/NCT03769506).

APCs bear important similarities to antibody–drug conjugates (ADCs), which have three components: a monoclonal antibody, a cytotoxic small-molecule drug, and a linker.[6] ADCs utilize the antigen specificity of monoclonal antibodies to deliver the therapeutic agent selectively to target tumors.[7–9] The physical and chemical properties of ADCs have been well-characterized, allowing for their translation into the clinical setting.[10,11] Some ADCs utilize light-sensitive functional groups such as anthracyclines,[12] duocarmycins,[13] and bacteriochlorins,[14] which may change the photostability of the conjugate. Furthermore, light-induced aggregation in photosensitive drug-bound ADCs has been demonstrated. For example, Cockrell et al. demonstrated that exposure of a trastuzumab–eosin photosensitizer conjugate to light induced aggregation.[15] The tendency for self-aggregation is an important predictor of ADC stability and efficacy,[16–18] and given the structural similarities, it is likely that APCs would be similarly subject to self-aggregation.

Received: May 17, 2020
Accepted: July 6, 2020
Published: July 6, 2020

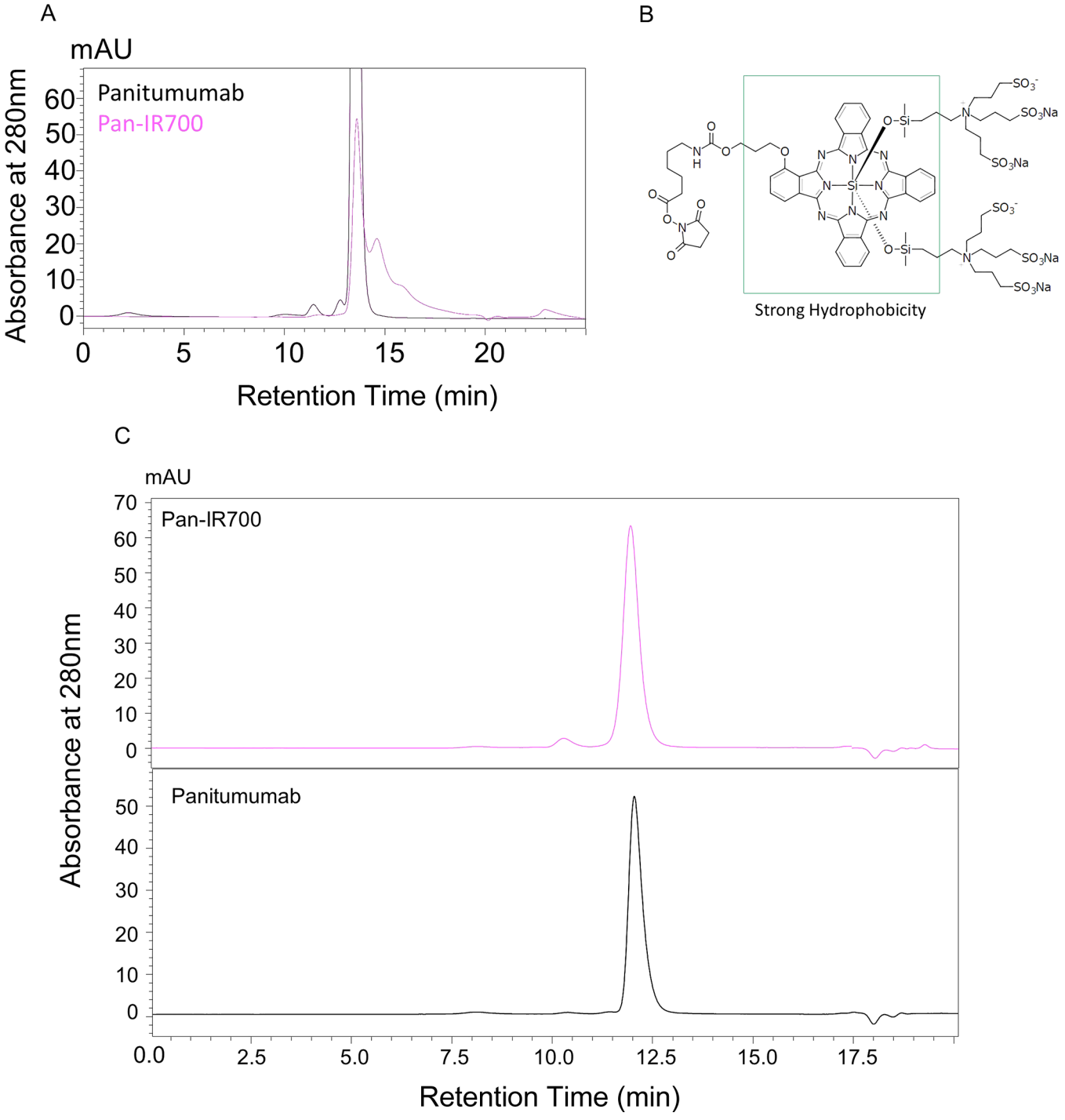

Figure 1. SEC analysis of panitumumab and Pan−IR700. (A) SEC analysis was performed using 200 mM phosphate buffer (pH 6.8) as a mobile phase. Poor separation was observed in the chromatogram of Pan−IR700. (B) Chemical structure of IR700. (C) SEC separation of Pan−IR700 was improved after 10% acetonitrile was added to the phosphate buffer.

Another key chemical and molecular property of an ADC is the amount of therapeutic drug (or photoabsorber, in the case of APCs) conjugated to the antibody, which affects the delivered dose as well as the drug's electrostatic surface charge, hydrophobicity, and likelihood of self-aggregation. Aggregation in particular is known also to depend on solvent properties such as salinity,[19] ionic strength,[20] and pH[21] and environmental factors such as temperature.[22]

While these properties are therefore likely to be important for the reproducibility and efficacy of NIR-PIT, they remain uninvestigated in APCs. Therefore, in this study we investigated the effect of IR700 load, light exposure, and solvent pH on APC chemical and physical properties, including stability. The model APC used in this study was panitumumab−IR700 (Pan−IR700), which is directed against EGFR-expressing cancer cells.

In order to evaluate the aggregation properties of Pan−IR700, the analytic conditions for size-exclusion chromatography (SEC) were optimized. Nonconjugated panitumumab and Pan−IR700 were analyzed under general SEC conditions

https://dx.doi.org/10.1021/acsmedchemlett.0c00262
ACS Med. Chem. Lett. 2020, 11, 1598−1604

using 200 mM phosphate buffer as a mobile phase. SEC chromatograms of these samples are shown in Figure 1A. The chromatogram of panitumumab showed a single peak eluting at 12 min. On the other hand, the chromatogram of Pan−IR700 showed a poor peak shape and incomplete resolution. Addition of 10% acetonitrile improved the separation of Pan−IR700, and the elution time of this monomer was almost the same as that of panitumumab (Figure 1C). Thus, all of the following examinations were performed using this analytical condition.

We evaluated the correlation between the IR700 loading and in vitro NIR-PIT efficacy. Figure 2A indicates that the percentage of PI-negative (i.e., viable) cells decreased with increasing IR700 loading up to an IR700-to-panitumumab ratio of 2.5:1, whereupon it reached a plateau at higher conjugation ratios. SEC analysis was performed for each agent (Figure 2B). Fluorescence quenching was observed at ratios above 2.5:1. These results indicated that an IR700-to-panitumumab ratio of 2.5:1 shows maximum cytotoxicity, suggesting that the number of cell-bound antibody molecules correlated with the antitumor effect of NIR-PIT but the number of IR700 molecules did not.

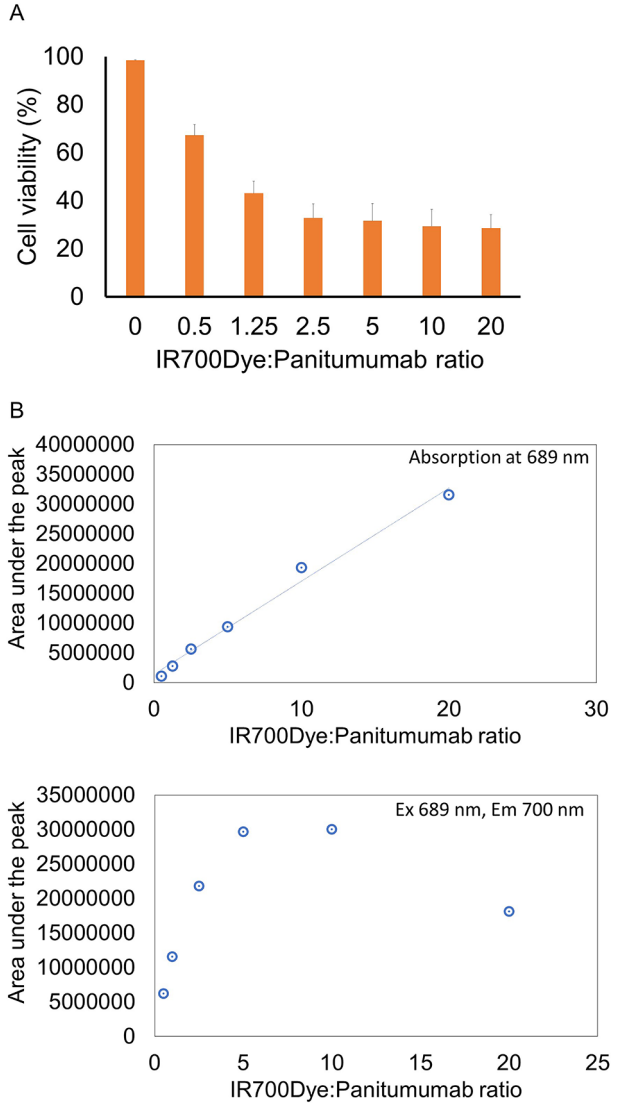

Figure 2. Effect of the IR700 loading. (A) Membrane damage and necrosis induced by NIR-PIT were measured by dead cell count using PI staining. Data are shown as means ± SEM. n = 4 in each group. (B) Plots of the absorption and fluorescence intensities of the monomer peak. Fluorescence quenching was observed at IR700:panitumumab ratios above 2.5:1.

In order to evaluate photoinduced aggregation, Pan−IR700 in a vial was illuminated with fluorescent light or LED light and then subjected to SEC analysis. Chromatograms displayed three peaks: a high-molecular-weight species (HMWS), monomer, and free dye. The monomer peak eluted slightly earlier with increasing light dose, possibly due to light-induced oligomer formation of mAb−IR700 initiated by single ligand release of $C_{14}H_{34}NO_{10}S_3Si$ from IR700. Such oligomers, which were identified as high-molecular-weight ladders on the SDS-PAGE gels in three different antibody−IR700 conjugates, including Pan−IR700,[3] would grow up to form aggregation upon a second ligand release reaction. Additionally, the area under the HMWS peak increased in a light-dose-dependent manner (Figure 3A). Figure 3B shows the change in the proportion of aggregates at each irradiation dose. It is worth noting that aggregation occurred with irradiation as low as 500 lx h. When light sources of different wavelengths were used, similar increases in water-soluble aggregates were observed.

The effect of pH on the stability of panitumumab and Pan−IR700 was evaluated using SEC analysis. Chromatograms of panitumumab (Figure 4A) show that no significant change occurred for 8 h under all pH conditions. On the other hand, chromatograms of Pan−IR700 (Figure 4B) show broadening and tailing of the monomer peak. In addition, an increase in the HMWS peak can also be seen. Time- and pH-dependent changes in aggregation are demonstrated in Figure 4C. Panitumumab was stable for 8 h under all pH conditions. In contrast, significant aggregation was observed over time in Pan−IR700 at pH 4, but the APC was stable at pH 5−8. To better understand the stability of Pan−IR700, deproteinized samples were analyzed using LC/MS/MS (Figure 4D,E). We detected a higher volume of released ligand ($C_{14}H_{34}NO_{10}S_3Si$) at pH 4 than at higher pH. These results suggested that acidic pH prompts ligand dissociation and results in aggregation of Pan−IR700 monomers.

Self-aggregation is an important parameter in quality control testing of antibody-based drugs. Aggregation may reduce the therapeutic efficacy, alter the pharmacokinetics, and increase the risk of an immunogenic drug reaction.[15] Therefore, we focused on APC aggregation properties in response to light irradiation and pH changes, which are especially important parameters in drug storage and administration.

SEC analysis of ADCs and APCs sometimes poses challenges because secondary interactions between the column and the drug conjugate are common. Experience from analysis of aggregates in ADC formulations tells us that the addition of an organic modifier such as dimethyl sulfoxide,[23] isopropyl alcohol,[24] propylene glycol,[25] or acetonitrile[26] can be used to decrease the nonspecific interactions between the stationary phase and the hydrophobic drug, thus reducing peak tailing and enhancing the resolution. In this study, adding 10% acetonitrile canceled out the hydrophobic interaction between the phthalocyanine of IR700 and the stationary phase of the column.

In general, the amount of drug loaded to an antibody−drug conjugate correlates positively with the therapeutic efficacy. However, while high drug loading can enhance the therapeutic effect, it also affects the stability and physical properties of the

https://dx.doi.org/10.1021/acsmedchemlett.0c00262
ACS Med. Chem. Lett. 2020, 11, 1598−1604

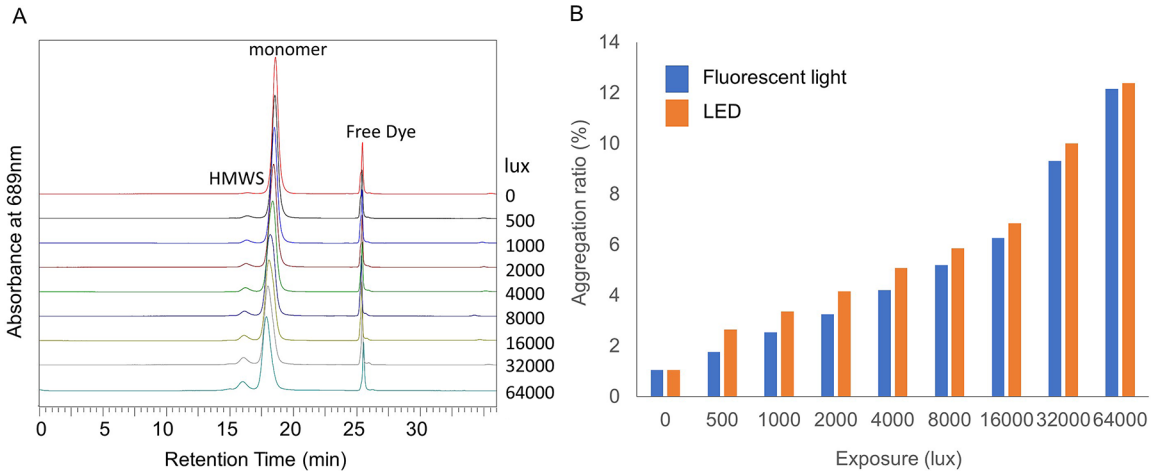

Figure 3. Evaluation of photoinduced aggregation. (A) SEC chromatograms showing the effect of fluorescent light irradiation. The high-molecular-weight species (HMWS) peak increased and the monomer peak tended to elute slightly earlier with increasing light irradiation. (B) The aggregation ratio of Pan−IR700 increased in a light-dose-dependent manner.

drug, sometimes resulting in decreased ADC activity.[27] In contrast, the unique mechanism of NIR-PIT allows that the IR700 load does not necessarily correlate with the therapeutic efficacy. While several previous studies have revealed the correlation between NIR light or mAb−IR700 dosage and antitumor effect in vitro and in vivo,[2,28] the effect of the IR700 conjugation ratio has never been reported. In this study, in vitro NIR-PIT efficacy was shown to increase with increased mixing ratio up to 2.5:1, after which no significant differences were observed in the proportion of PI-negative (i.e., viable) cells (Figure 2A).

Second, we characterized the fluorescence intensity of Pan−IR700. Fluorescence quenching occurs by fluorescence resonance energy transfer (FRET), contact quenching, or collisional quenching due to high concentrations.[29,30] Here, fluorescence quenching was observed in mixing ratios above 2.5:1. Interestingly, we note a correlation between the trends in fluorescence quenching and NIR-PIT efficacy,[3] and therefore, fluorescence quenching measurements could be used to determine the optimum amount of IR700 in future studies.

Previous studies have shown that NIR-PIT occurs not only in near-infrared light[1,2,31] but also in short-wavelength light such as Cerenkov light.[32] However, there have been no reports that evaluated APC photoreactivity in room light. Here we have shown that Pan−IR700 aggregates in only an hour with 500 lx irradiation which is almost the same illuminance as with room light (Figure 3). These results indicate that this is a very light-sensitive substance, and drug storage and administration protocols would therefore likely benefit by aiming to keep APCs in opaque containers until immediately before administration. Furthermore, contamination of aggregates could pose a safety risk to patients[18] and should therefore be handled with caution during manufacture, storage, and administration.

The effects of pH on the stability of APCs are also important, especially in clinical use, because the pH of buffered solutions for drip infusions can vary from pH 4 to 8. In this study, we have demonstrated that panitumumab showed no aggregation nor denaturation in 8 h across multiple pH values. In contrast, Pan−IR700 significantly aggregated and denatured in just 1 h under acidic conditions, and LC/MS/MS analysis confirmed that IR700 degraded at pH 4. Under acidic conditions, the siloxane bond between the phthalocyanine and the ligand is likely hydrolyzed (Figure 4F). This reaction increases the hydrophobicity of Pan−IR700, resulting in aggregation and denaturation. These results suggest that acidic solutions negatively affect the APC stability, which could have implications during manufacturing.

One of the limitations of this study is that size-exclusion chromatography using UV/PDA detectors can only evaluate changes in water-soluble aggregates. Evaluation of water-insoluble aggregates such as subvisible particles using dynamic light scattering[33] might enhance our understanding of the aggregation properties of the APC. In addition, a fuller understanding of the effects of variations in concentration, type of antibody, and temperature are required in future studies.

In conclusion, this is the first study to evaluate several important physicochemical properties of APCs for NIR-PIT, including (1) IR700-to-antibody conjugation ratio and its effect on therapeutic efficacy, (2) the effect of the ambient light irradiation dose on APC aggregation, and (3) the effect of solvent pH on APC degeneration and aggregation. Attention should be devoted to minimizing variations in these parameters, especially during vulnerable steps in the process, such as drug synthesis, packaging, and storage. Our results indicate that small variations in these parameters can have significant effects on drug efficacy and stability, and consistent manufacturing and storage protocols in the future will likely help to minimize patient safety risks and improve therapeutic efficacy.

EXPERIMENTAL PROCEDURES

Chemicals and Reagents. The water-soluble silica−phthalocyanine dye IRDye 700DX NHS ester ($C_{74}H_{96}N_{12}Na_4O_{27}S_6Si_3$, molecular weight = 1954.22) was purchased from LI-COR Bioscience (Lincoln, NE). A fully humanized IgG2 monoclonal antibody (mAb) against human epidermal growth factor receptor (hEGFR), panitumumab, was purchased from Amgen (Thousand Oaks, CA). All other chemicals were reagent-grade.

Synthesis of IR700-Conjugated Panitumumab (Pan−IR700). Panitumumab was conjugated to IR700 according to a previously published protocol.[34] The conjugated antibody was purified using a Sephadex G50 column (PD-10, GE Healthcare) and filtered using a 0.22 μm PVDF syringe filter (Millipore). All operations were performed in a dark room of 200 lx or less. The antibody concentration was measured by the absorption at 280 nm (8453

https://dx.doi.org/10.1021/acsmedchemlett.0c00262
ACS Med. Chem. Lett. 2020, 11, 1598−1604

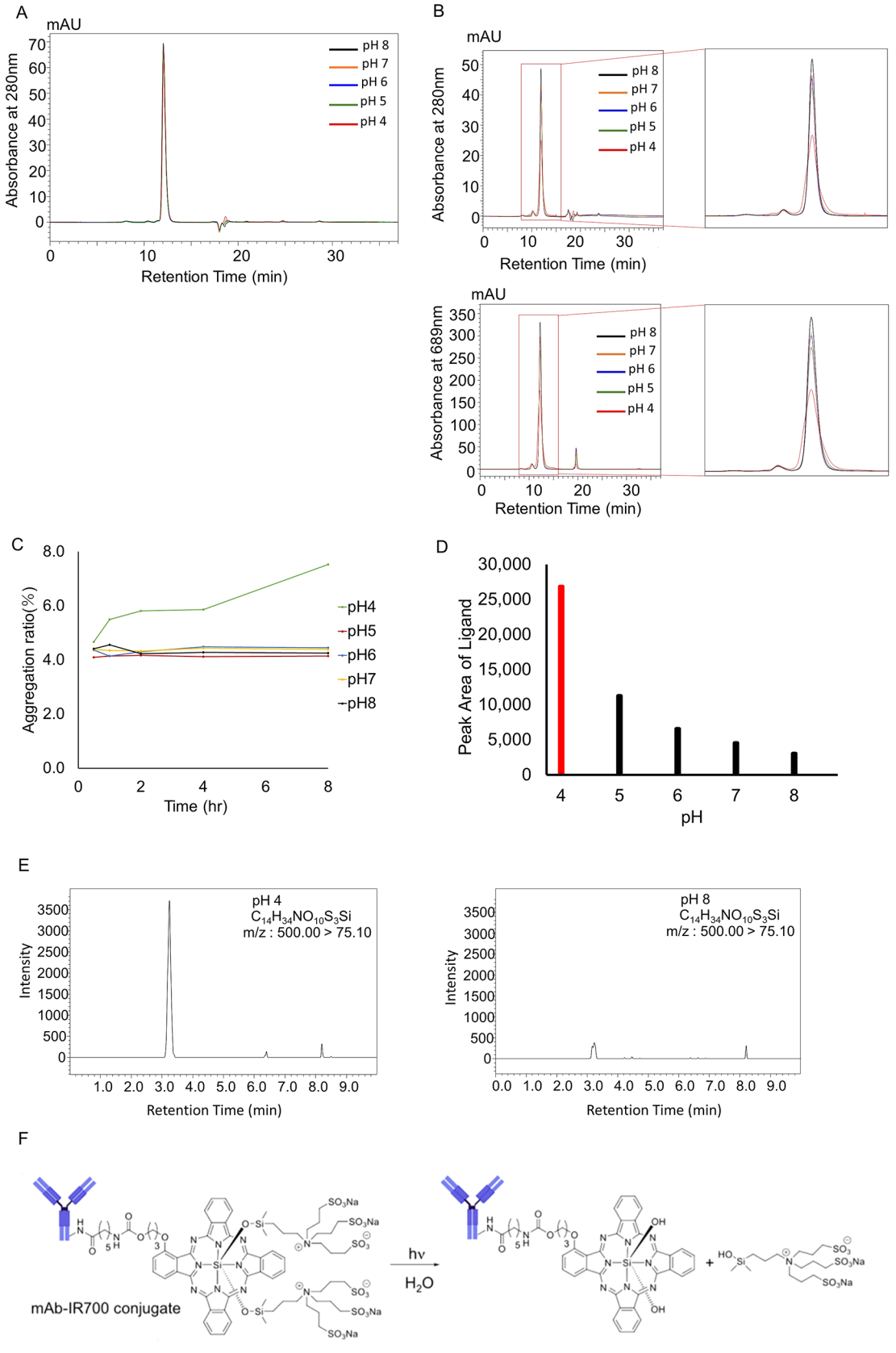

Figure 4. Effect of solvent pH. (A) SEC chromatograms of panitumumab. No specific changes were visually observed at any pH after incubation for 8 h. (B) SEC chromatograms of Pan−IR700 at 280 nm and 689 nm. An increase in the HMWS peak was observed at pH 4 after incubation for 8 h. (C) Plots of the increase in the amount of aggregation vs incubation time at different pH values. The amount of aggregation increased over time at pH 4. (D) LC/MS/MS detected release of the ligand after incubation for 8 h at pH 4. (E) Ligand peak intensities of samples at different pH after incubation for 8 h. The ligand peak was significantly higher at pH 4. (F) Hypothesized change of chemical structure of Pan−IR700 under acidic conditions.

https://dx.doi.org/10.1021/acsmedchemlett.0c00262
ACS Med. Chem. Lett. 2020, 11, 1598−1604

Value System, Agilent Technologies). Similarly, the amount of conjugated IR700 was determined by the absorption at 689 nm.

Size-Exclusion Chromatography. For the systemic evaluation of stability, SEC was performed using a Shimadzu Nexera XR HPLC system. TSKgel UltraSW Aggregate (7.8 mm × 300 mm, 3 μm; Tosoh Bioscience) with a TSKgel guard column UltraSW (6.0 mm × 40 mm, 3 μm; Tosoh Bioscience) was used for separation of the APCs by size. The mobile phase was composed of a 200 mM sodium phosphate buffer (pH 6.8).

Acetonitrile (10%) was added to the sodium phosphate buffer. Approximately 25 μg of each sample was injected onto the column without dilution. The absorbance at 280 and 689 nm was monitored by a SPD-M30A PDA detector. We also monitored the excitation wavelength at 689 nm and the emission wavelength at 700 nm using an RF-20 Axs detector. Data were processed using Shimadzu Labsolutions software.

Effect of IR700 Loading. In order to evaluate the effect of the IR700 loading, six samples with different IR700:panitumumab mixing ratios (0:1, 0.5:1, 1.25:1, 2.5:1, 5:1, 10:1, 20:1) were prepared. These samples were analyzed using SEC, and the monomer peak areas at the absorption wavelength and fluorescence wavelengths of IR700 were plotted. The therapeutic effect of each sample was evaluated by in vitro NIR-PIT as described below.

Cell Culture. A431 luciferase cells expressing hEGFR were grown in RPMI-1640 medium supplemented with 10% fetal bovine serum and 1% penicillin streptomycin in tissue culture flasks in a humidified incubator at 37 °C in an atmosphere of 5% carbon dioxide and 95% air.

In Vitro NIR-PIT. The cytotoxic effects of NIR-PIT were determined by flow cytometry analysis. A431 cells (2×10^5) were seeded into 12-well plates and incubated for 24 h. The medium was replaced with fresh culture medium containing 10 μg/mL APC, followed by incubation for 3 h at 37 °C. Cells were washed with PBS and then irradiated with an NIR (690 nm) laser (ML7710, Modulight Inc.) at a power density of 4 J/cm^2. Cells were detached 1 h after irradiation, and propidium iodide (PI) was added. Samples were analyzed by flow cytometry (FACSCalibur, BD Biosciences).

Evaluation of Photoinduced Aggregation. In order to evaluate the photostability of Pan−IR700, a fluorescent light (318C3 45 W fluorescent light with a 6500 K daylight bulb, Dazor Lighting Technology) or an LED light (L1570 LED desk light, Dazor Lighting Technology), which have a color temperature of 6500 K, was used to illuminate each sample at 500 lx h. The illuminance of each light source was measured with an illuminometer. A 1 mL aliquot of Pan−IR700 (500 μg/mL) was dispensed into each vial, and three vials were prepared for each irradiation condition. Samples were irradiated with 0, 500, 1000, 2000, 4000, 8000, 16 000, 32 000, or 64 000 lx h and subsequently analyzed by SEC. The aggregation ratio of each sample was calculated with the following equation:

$$\%\ \text{aggregation} = \frac{\text{area of aggregate peak}}{\text{area of all peaks}} \times 100$$

Effect of Solvent pH. Phosphate buffer solutions (100 mM, covering a pH range of 6.0−8.0) and acetate buffer (100 mM, covering a pH range of 4.0−5.0) were prepared. Panitumumab and Pan−IR700 solutions (500 μg/mL) were mixed with an equal volume of each buffer and incubated at 25 °C under shielded conditions for a period of 8 h. The pH after mixing was measured with a pH monitor by mixing blank PBS and each buffer solution. These samples were withdrawn at time intervals of 0.5, 1, 2, 4, and 8 h and then analyzed using SEC. To better understand the effect of pH, we performed LC/MS analysis. Each sample was diluted 5-fold with 1% formic acid in methanol. After centrifugation at 14 000 rpm at 4 °C for 10 min, the supernatants were transferred into new tubes. LC/MS analysis was performed on a liquid chromatograph mass spectrometer (LCMS-8050, Shimadzu) as described in previous work.[5]

AUTHOR INFORMATION

Corresponding Author

Hisataka Kobayashi − *Molecular Imaging Program, Center for Cancer Research, National Cancer Institute, National Institutes of Health, Bethesda, Maryland 20892, United States;* orcid.org/0000-0003-1019-4112; Phone: 240-858-3069; Email: kobayash@mail.nih.gov; Fax: 240-541-4527

Authors

Daiki Fujimura − *Molecular Imaging Program, Center for Cancer Research, National Cancer Institute, National Institutes of Health, Bethesda, Maryland 20892, United States*

Fuyuki Inagaki − *Molecular Imaging Program, Center for Cancer Research, National Cancer Institute, National Institutes of Health, Bethesda, Maryland 20892, United States*

Ryuhei Okada − *Molecular Imaging Program, Center for Cancer Research, National Cancer Institute, National Institutes of Health, Bethesda, Maryland 20892, United States*

Adrian Rosenberg − *Molecular Imaging Program, Center for Cancer Research, National Cancer Institute, National Institutes of Health, Bethesda, Maryland 20892, United States*

Aki Furusawa − *Molecular Imaging Program, Center for Cancer Research, National Cancer Institute, National Institutes of Health, Bethesda, Maryland 20892, United States*

Peter L. Choyke − *Molecular Imaging Program, Center for Cancer Research, National Cancer Institute, National Institutes of Health, Bethesda, Maryland 20892, United States*

Complete contact information is available at: https://pubs.acs.org/10.1021/acsmedchemlett.0c00262

Author Contributions

D.F. mainly designed and conducted experiments, performed analysis, and wrote the manuscript; F.I., R.O., and A.F. performed experiments and analysis; A.R. and P.L.C. edited the manuscript and supervised the project; and H.K. planned and initiated the project, designed and conducted experiments, wrote the manuscript, and supervised the entire project.

Notes

The authors declare no competing financial interest.

ACKNOWLEDGMENTS

This research was supported by the Intramural Research Program of the National Institutes of Health, National Cancer Institute, Center for Cancer Research (ZIA BC 011513). F.I. was also supported by a grant from the National Center for Global Health and Medicine Research Institute, Tokyo, Japan. For A.R., this research was made possible through the NIH Medical Research Scholars Program, a public−private partnership supported jointly by the NIH and contributions to the Foundation for the NIH.

REFERENCES

(1) Kobayashi, H.; Choyke, P. L. Near-Infrared Photoimmunotherapy of Cancer. *Acc. Chem. Res.* **2019**, *52* (8), 2332−2339.

(2) Mitsunaga, M.; Ogawa, M.; Kosaka, N.; Rosenblum, L. T.; Choyke, P. L.; Kobayashi, H. Cancer cell-selective in vivo near infrared photoimmunotherapy targeting specific membrane molecules. *Nat. Med.* **2011**, *17* (12), 1685−91.

(3) Sato, K.; Ando, K.; Okuyama, S.; Moriguchi, S.; Ogura, T.; Totoki, S.; Hanaoka, H.; Nagaya, T.; Kokawa, R.; Takakura, H.; Nishimura, M.; Hasegawa, Y.; Choyke, P. L.; Ogawa, M.; Kobayashi, H. Photoinduced Ligand Release from a Silicon Phthalocyanine Dye Conjugated with Monoclonal Antibodies: A Mechanism of Cancer

Cell Cytotoxicity after Near-Infrared Photoimmunotherapy. *ACS Cent. Sci.* **2018**, *4* (11), 1559−1569.
(4) Mitsunaga, M.; Nakajima, T.; Sano, K.; Kramer-Marek, G.; Choyke, P. L.; Kobayashi, H. Immediate in vivo target-specific cancer cell death after near infrared photoimmunotherapy. *BMC Cancer* **2012**, *12*, 345.
(5) Ogawa, M.; Tomita, Y.; Nakamura, Y.; Lee, M. J.; Lee, S.; Tomita, S.; Nagaya, T.; Sato, K.; Yamauchi, T.; Iwai, H.; Kumar, A.; Haystead, T.; Shroff, H.; Choyke, P. L.; Trepel, J. B.; Kobayashi, H. Immunogenic cancer cell death selectively induced by near infrared photoimmunotherapy initiates host tumor immunity. *Oncotarget* **2017**, *8* (6), 10425−10436.
(6) Kobayashi, H.; Griffiths, G. L.; Choyke, P. L. Near-Infrared Photoimmunotherapy: Photoactivatable Antibody−Drug Conjugates (ADCs). *Bioconjugate Chem.* **2020**, *31* (1), 28−36.
(7) Hamann, P. R.; Hinman, L. M.; Hollander, I.; Beyer, C. F.; Lindh, D.; Holcomb, R.; Hallett, W.; Tsou, H. R.; Upeslacis, J.; Shochat, D.; Mountain, A.; Flowers, D. A.; Bernstein, I. Gemtuzumab ozogamicin, a potent and selective anti-CD33 antibody−calicheamicin conjugate for treatment of acute myeloid leukemia. *Bioconjugate Chem.* **2002**, *13* (1), 47−58.
(8) Larson, R. A.; Sievers, E. L.; Stadtmauer, E. A.; Lowenberg, B.; Estey, E. H.; Dombret, H.; Theobald, M.; Voliotis, D.; Bennett, J. M.; Richie, M.; Leopold, L. H.; Berger, M. S.; Sherman, M. L.; Loken, M. R.; van Dongen, J. J.; Bernstein, I. D.; Appelbaum, F. R. Final report of the efficacy and safety of gemtuzumab ozogamicin (Mylotarg) in patients with CD33-positive acute myeloid leukemia in first recurrence. *Cancer* **2005**, *104* (7), 1442−52.
(9) LoRusso, P. M.; Weiss, D.; Guardino, E.; Girish, S.; Sliwkowski, M. X. Trastuzumab emtansine: a unique antibody−drug conjugate in development for human epidermal growth factor receptor 2-positive cancer. *Clin. Cancer Res.* **2011**, *17* (20), 6437−47.
(10) Beck, A.; Goetsch, L.; Dumontet, C.; Corvaia, N. Strategies and challenges for the next generation of antibody−drug conjugates. *Nat. Rev. Drug Discovery* **2017**, *16* (5), 315−337.
(11) Gandhi, A. V.; Arlotta, K. J.; Chen, H. N.; Owen, S. C.; Carpenter, J. F. Biophysical Properties and Heating-Induced Aggregation of Lysine-Conjugated Antibody−Drug Conjugates. *J. Pharm. Sci.* **2018**, *107* (7), 1858−1869.
(12) Chen, X.; Ding, G.; Gao, Q.; Sun, J.; Zhang, Q.; Du, L.; Qiu, Z.; Wang, C.; Zheng, F.; Sun, B.; Ni, J.; Feng, Z.; Zhu, J. A human anti-c-Met Fab fragment conjugated with doxorubicin as targeted chemotherapy for hepatocellular carcinoma. *PLoS One* **2013**, *8* (5), No. e63093.
(13) Ducry, L.; Stump, B. Antibody−drug conjugates: linking cytotoxic payloads to monoclonal antibodies. *Bioconjugate Chem.* **2010**, *21* (1), 5−13.
(14) Pye, H.; Stamati, I.; Yahioglu, G.; Butt, M.; Deonarain, M. Antibody-directed phototherapy (ADP). *Antibodies* **2013**, *2* (2), 270−305.
(15) Cockrell, G. M.; Wolfe, M. S.; Wolfe, J. L.; Schoneich, C. Photoinduced aggregation of a model antibody−drug conjugate. *Mol. Pharmaceutics* **2015**, *12* (6), 1784−97.
(16) Ahmadi, M.; Bryson, C. J.; Cloake, E. A.; Welch, K.; Filipe, V.; Romeijn, S.; Hawe, A.; Jiskoot, W.; Baker, M. P.; Fogg, M. H. Small amounts of sub-visible aggregates enhance the immunogenic potential of monoclonal antibody therapeutics. *Pharm. Res.* **2015**, *32* (4), 1383−94.
(17) Langille, S. E. Particulate matter in injectable drug products. *PDA J. Pharm. Sci. Technol.* **2013**, *67* (3), 186−200.
(18) Rosenberg, A. S. Effects of protein aggregates: an immunologic perspective. *AAPS J.* **2006**, *8* (3), E501−7.
(19) Kastelic, M.; Kalyuzhnyi, Y. V.; Hribar-Lee, B.; Dill, K. A.; Vlachy, V. Protein aggregation in salt solutions. *Proc. Natl. Acad. Sci. U. S. A.* **2015**, *112* (21), 6766−70.
(20) Sahin, E.; Grillo, A. O.; Perkins, M. D.; Roberts, C. J. Comparative effects of pH and ionic strength on protein−protein interactions, unfolding, and aggregation for IgG1 antibodies. *J. Pharm. Sci.* **2010**, *99* (12), 4830−48.
(21) Mohamed, H. E.; Mohamed, A. A.; Al-Ghobashy, M. A.; Fathalla, F. A.; Abbas, S. S. Stability assessment of antibody−drug conjugate Trastuzumab emtansine in comparison to parent monoclonal antibody using orthogonal testing protocol. *J. Pharm. Biomed. Anal.* **2018**, *150*, 268−277.
(22) Li, Y.; Ogunnaike, B. A.; Roberts, C. J. Multi-variate approach to global protein aggregation behavior and kinetics: effects of pH, NaCl, and temperature for alpha-chymotrypsinogen A. *J. Pharm. Sci.* **2010**, *99* (2), 645−62.
(23) Schellinger, A. P.; Stoll, D. R.; Carr, P. W. High speed gradient elution reversed-phase liquid chromatography. *J. Chromatogr A* **2005**, *1064* (2), 143−56.
(24) Striegel, A. M.; Yau, W. W.; Kirkland, J. J.; Bly, D. D. *Modern Size-Exclusion Liquid Chromatography: Practice of Gel Permeation and Gel Filtration Chromatography*, 2nd ed.; John Wiley & Sons: Hoboken, NJ, 2009.
(25) Davis, J. M.; Stoll, D. R. Likelihood of total resolution in selective comprehensive two-dimensional liquid chromatography with parallel processing: Simulation and theory. *J. Chromatogr A* **2018**, *1537*, 43−57.
(26) Stoll, D. R.; Shoykhet, K.; Petersson, P.; Buckenmaier, S. Active Solvent Modulation: A Valve-Based Approach To Improve Separation Compatibility in Two-Dimensional Liquid Chromatography. *Anal. Chem.* **2017**, *89* (17), 9260−9267.
(27) Buecheler, J. W.; Winzer, M.; Tonillo, J.; Weber, C.; Gieseler, H. Impact of Payload Hydrophobicity on the Stability of Antibody−Drug Conjugates. *Mol. Pharmaceutics* **2018**, *15* (7), 2656−2664.
(28) Nakajima, T.; Sato, K.; Hanaoka, H.; Watanabe, R.; Harada, T.; Choyke, P. L.; Kobayashi, H. The effects of conjugate and light dose on photo-immunotherapy induced cytotoxicity. *BMC Cancer* **2014**, *14*, 389.
(29) Kobayashi, H.; Choyke, P. L. Target-cancer-cell-specific activatable fluorescence imaging probes: rational design and in vivo applications. *Acc. Chem. Res.* **2011**, *44* (2), 83−90.
(30) Kobayashi, H.; Ogawa, M.; Alford, R.; Choyke, P. L.; Urano, Y. New strategies for fluorescent probe design in medical diagnostic imaging. *Chem. Rev.* **2010**, *110* (5), 2620−40.
(31) Okuyama, S.; Nagaya, T.; Sato, K.; Ogata, F.; Maruoka, Y.; Choyke, P. L.; Kobayashi, H. Interstitial near-infrared photoimmunotherapy: effective treatment areas and light doses needed for use with fiber optic diffusers. *Oncotarget* **2018**, *9* (13), 11159−11169.
(32) Nakamura, Y.; Nagaya, T.; Sato, K.; Okuyama, S.; Ogata, F.; Wong, K.; Adler, S.; Choyke, P. L.; Kobayashi, H. Cerenkov Radiation-Induced Photoimmunotherapy with (18)F-FDG. *J. Nucl. Med.* **2017**, *58* (9), 1395−1400.
(33) Rowe, J. B.; Flynn, R. P.; Wooten, H. R.; Noufer, H. A.; Cancel, R. A.; Zhang, J.; Subramony, J. A.; Pechenov, S.; Wang, Y. Submicron Aggregation of Chemically Denatured Monoclonal Antibody. *Mol. Pharmaceutics* **2018**, *15* (10), 4710−4721.
(34) Sato, K.; Watanabe, R.; Hanaoka, H.; Harada, T.; Nakajima, T.; Kim, I.; Paik, C. H.; Choyke, P. L.; Kobayashi, H. Photoimmunotherapy: comparative effectiveness of two monoclonal antibodies targeting the epidermal growth factor receptor. *Mol. Oncol.* **2014**, *8* (3), 620−32.

https://dx.doi.org/10.1021/acsmedchemlett.0c00262
ACS Med. Chem. Lett. 2020, 11, 1598−1604